POLITECNICO DI TORINO
Repository ISTITUZIONALE

Adaptive Stokes-Based Polarization Demultiplexing for Long-Haul Multi-Subcarrier Systems

Original
Adaptive Stokes-Based Polarization Demultiplexing for Long-Haul Multi-Subcarrier Systems / Ziaie, S., Guiomar, F.P., Muga, N.J., Nespola, A., Bosco, G., Carena, A., Pinto, A.N.. - In: IEEE PHOTONICS TECHNOLOGY LETTERS. - ISSN 1041-1135. - STAMPA. - 31:10(2019), pp. 759-762. [10.1109/LPT.2019.2906858]

Availability:
This version is available at: 11583/2742117 since: 2019-07-16T13:15:47Z

Publisher:
Institute of Electrical and Electronics Engineers Inc.

Published
DOI:10.1109/LPT.2019.2906858

Terms of use:

This article is made available under terms and conditions as specified in the corresponding bibliographic description in the repository

Publisher copyright

(Article begins on next page)

08 October 2026

This article has been accepted for publication in a future issue of this journal, but has not been fully edited. Content may change prior to final publication. Citation information: DOI 10.1109/LPT.2019.2906858, IEEE Photonics Technology Letters

Adaptive Stokes-Based Polarization Demultiplexing for Long-Haul Multi-Subcarrier Systems

Somayeh Ziaie, Fernando P. Guiomar, Nelson J. Muga, Antonino Nespola, Gabriella Bosco, Andrea Carena and Armando N. Pinto

***Abstract*—We experimentally evaluate the performance of the adaptive Stokes polarization demultiplexing (PolDemux) algorithm over a long-haul optical link considering the propagation of 31×192 Gb/s channels modulated as PM-16QAM multi-subcarrier (MSC) signals. Initially, we consider 1×24 Gbaud channel under test, and subsequently we assess the performance of the algorithm on an increasing number of subcarriers (up to 12×2 Gbaud) while keeping the same aggregate symbol rate. Taking advantage of the higher robustness of MSC signals towards chromatic dispersion (CD), we demonstrate that the memoryless Stokes-based PolDemux algorithm, originally designed for short reach links, can also be used for low-complexity and modulation transparent polarization demultiplexing in long-haul systems. In addition, we demonstrate that the PolDemux rotation matrix for MSC signals can be estimated over a restricted group of N_{ref} subcarriers and seamlessly applied to all N_{sc} subcarriers, thereby significantly reducing the overall complexity by a factor of $\sim N_{\mathrm{sc}}/N_{\mathrm{ref}}$.**

***Index Terms*—Subcarrier multiplexing, Stokes space, coherent detection, polarization demultiplexing.**

I. Introduction

In coherent optical systems assisted by digital signal processing (DSP), high spectral efficiency transmission is enabled by the use of high-order modulation formats together with polarization multiplexing (PM). This requires robust and high performance polarization demultiplexing (PolDemux) at the receiver-side, independently of the modulation format.

Although the constant modulus algorithm (CMA) is an attractive solution for constant amplitude formats, its extension to multi-level QAM modulation requires a radius-directed equalization (RDE) strategy, which is modulation format dependent and may require several cascaded training stages for proper pre-convergence [1]. In addition, this class of PolDemux algorithms generally suffers from the well-known problem of singularity, resulting in the loss of information on one polarization [2]. To circumvent these limitations, a three-dimensional (3-D) adaptive Stokes space PolDemux algorithm was proposed as a format transparent and low-complexity technique, which is singularity-free and provides faster convergence [3], [4]. However, the performance of the memoryless Stokes PolDemux can be significantly degraded by memory effects [3], which are mostly due to residual chromatic dispersion (CD). For this reason, the application of this algorithm has been so far limited to short-reach systems [4]. In the context of long-haul optical systems, it has been recently demonstrated that digital multi-subcarrier (MSC) modulation enables to efficiently improve the nonlinear transmission performance, providing up to 20% increased propagation reach with no additional DSP overhead [5], [6]. Furthermore, at the typical optimum symbol-rates per subcarrier of 2–6 Gbaud, the system also benefits from higher tolerance towards CD comparing with traditional single-carrier systems ($\geq$32 Gbaud) [7]. Under these circumstances, it is of great interest to test the application of the Stokes PolDemux approach with MSC modulation, providing a format-agnostic PolDemux solution for long-haul transmission systems.

Benefiting from the fact that wideband MSC signals are actually composed of several narrowband subcarriers, which enhances its robustness against CD [7], we experimentally demonstrate for the first time to our knowledge the implementation of Stokes-based PolDemux for long-haul optical transmission ($>$ 2000 km). In addition, by observing that the polarization rotation is strongly correlated between subcarriers, we demonstrate that the complexity of PolDemux for MSC signals can be substantially reduced. This is achieved by performing polarization rotation monitoring over a subset of N_{ref} reference subcarriers, and then applying the extracted PolDemux rotation matrices to the remaining N_{sc} subcarriers, in groups of $N_{\mathrm{sc}}/N_{\mathrm{ref}}$ nearest neighbor subcarriers. Moreover, we experimentally assess the requirements in terms of CD compensation precision for penalty-free Stokes PolDemux, while demonstrating its compatibility with the well-known symbol rate optimization (SRO) benefit in MSC systems.

II. Extending Stokes PolDemux to MSC Signals

The adaptive Stokes algorithm proposed in [3] can be divided into two stages, as shown in Fig. 1. The first stage corresponds to the cascade of sub-stages that go from the computation of the Stokes parameters of the received data to the estimation of the inverse state of polarization (SOP) rotation matrix, which we designate as polarization tracking (PolTrack). After representing the received data in the Stokes space, the algorithm finds a best fitting plane,

This work was supported in part by Fundação para a Ciência e a Tecnologia (FCT) through national funds and when applicable co-funded by FEDER-PT2020 partnership agreement under the projects UID/EEA/50008/2013 (action SoftTransceiver and Optical-5G), and DSPMetroNet (POCI-01-0145-FEDER-029405) and PhD grant SFRH/BD/120665/2016, and through the Regional Operational Programme of Centre (CENTRO 2020) of the Portugal 2020 framework, project ORCIP (CENTRO-01-0145-FEDER-022141).

S. Ziaie, F. P. Guiomar, N. J. Muga and A. N. Pinto are with the Department of Electronic, Telecommunications, and Informatics, University of Aveiro, and also with the Instituto de Telecomunicações, Campus Universitário de Santiago, 3810-193 Aveiro, Portugal (e-mail: sziaie@ua.pt)

A. Nespola is with Istituto Superiore Mario Boella, via Pier Carlo Boggio 61, 10138 Torino, Italy (e-mail: nespola@ismb.it)

G. Bosco and A. Carena are with Dipartimento di Elettronica e Telecomunicazioni, Politecnico di Torino, Corso Duca degli Abruzzi, 24, 10129 Torino, Italy (e-mail: andrea.carena@polito.it)

1041-1135 (c) 2018 IEEE. Personal use is permitted, but republication/redistribution requires IEEE permission. See http://www.ieee.org/publications_standards/publications/rights/index.html for more information.

This article has been accepted for publication in a future issue of this journal, but has not been fully edited. Content may change prior to final publication. Citation information: DOI 10.1109/LPT.2019.2906858, IEEE Photonics Technology Letters

whose normal is then employed in the computation of the transformation matrix capable of reversing the mixing of the two orthogonal polarization components [3]. The algorithm uses the Stokes vector of each sample, $\hat{s}(k+1)$, to continuously compute the normal $\hat{n}(k+1)$. Sample by sample, and agnostically to the modulation format, the orientation of the normal $\hat{n}(k)$ is therefore updated following the rule,

$$\hat{n}(k+1) = (\hat{n}(k) + \vec{\Gamma}(k+1))B, \tag{1}$$

where B represents a normalization factor, and k is the sample number. $\vec{\Gamma}(k+1)$ represents a vector lying in the Stokes plane with direction perpendicular to $\hat{s}(k+1)$,

$$\vec{\Gamma}(k+1) = \mu A[\hat{s}(k+1) \times \hat{n}(k)] \times \hat{s}(k+1), \tag{2}$$

where μ is the step-size parameter and $A = |\hat{s}(k) \cdot \hat{n}(k)|$. The $\hat{s}(k+1)$ is the Stokes vector representing the SOP of the optical field at sample $k+1$. The inverse SOP rotation matrix $F(\hat{n}(k))$ can be calculated as,

$$\mathbf{F} = \begin{bmatrix} \cos(p)\exp(i\,q/2) & \sin(p)\exp(-i\,q/2) \\ -\sin(p)\exp(i\,q/2) & \cos(p)\exp(-i\,q/2) \end{bmatrix} \tag{3}$$

where $p = 1/2\,\mathrm{atan}(a, (b^2+c^2)^{1/2})$ and $q = \mathrm{atan}(b, c)$, with a, b and c representing the normal vector components, $\hat{n}(k) = (a, b, c)^T$ in the Stokes space [3]. The second stage of the algorithm consists of the polarization rotation (PolRot) part, which basically corresponds to the multiplication of the incoming signal by the previously estimated SOP rotation matrix of expression (3) [3]. For each polarization-multiplexed component, x_{in} and y_{in}, the PolRot output signals, x_{out} and y_{out}, are calculated as $x_{out}/y_{out} = f_{xx/yx}x_{in} + f_{xy/yy}y_{in}$, where f_{xx}, f_{xy}, f_{yx} and f_{yy} are the complex-valued scalar components of the inverse SOP rotation matrix $\mathbf{F}$.

As can be easily perceived, most of the complexity of the Stokes PolDemux algorithm lies in the PolTrack stage, which includes several trigonometric operations and multiplications. Moreover, the process of adaptively finding the best fitting plan and normal vectors also introduces some processing latency, as it requires a minimum convergence time. In contrast, the PolRot stage is actually very simple, as it requires only 8 real multiplications and 6 additions per polarization. Therefore, it can be safely stated that the complexity of the PolTrack stage is much larger than the complexity of the PolRot stage.

Thus, the overall complexity of Stokes PolDemux can be significantly reduced by narrowing the bandwidth over which PolTrack is performed. Taking advantage of the subcarrier multiplexing concept, this can be seamlessly done by selecting just a few designated reference subcarriers for the application

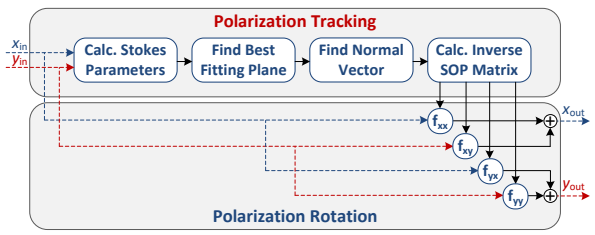

Fig. 1. Schematic representation of the adaptive Stokes PolDemux algorithm.

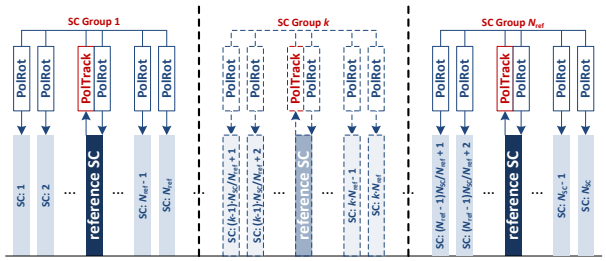

Fig. 2. Applying the Stokes PolDemux over an MSC signal, using a subset of N_{ref} reference subcarriers for polarization tracking.

of the PolTrack stage. The proposed reduced complexity Stokes PolDemux is illustrated in Fig. 2. The MSC signal is first divided into N_{ref} groups of $N_{\mathrm{sc}}/N_{\mathrm{ref}}$ subcarriers, where PolTrack stage is applied only over a reference (central) subcarrier, and the PolRot stage is then applied equally to all subcarriers within the same group. The total number of reference subcarriers can be adjusted based on the performance requirements. Assuming that the complexity of PolTrack is largely dominant, it therefore becomes apparent that this strategy enables to approximately reduce the overall PolDemux complexity by a factor of $N_{\mathrm{sc}}/N_{\mathrm{ref}}$.

III. Experimental Setup and DSP Subsystems

The experimental setup depicted in Fig. 3 has been used to validate the performance of Stokes PolDemux implemented in a long-haul optical link, transmitting 31 WDM channels with spacing of 28 GHz. Each optical channel is composed of root raised-cosine (0.05 roll-off) PM-16QAM MSC signals with an aggregate symbol-rate of $R_{\mathrm{s}} = 24$ Gbaud and variable number of subcarriers, $N_{\mathrm{sc}} \in [1, 2, 4, 6, 8, 12]$, with an inter-subcarrier spacing of $1.05\times R_{\mathrm{s}}/N_{\mathrm{sc}}$. Each 16QAM subcarrier carries bit-level information originated by uncorrelated pseudo-random bit sequence (PRBS), with length varying between 2^{15} (highest symbol-rate) and 2^{11} (lowest symbol-rate) symbols. For each optical channel, the digital MSC signal, including pre-emphasis, is converted to an analog electrical signal by a 64 Gsa/s digital-to-analog converter (DAC). The channel under test (CUT) is generated using an external cavity laser (ECL) with $<$100 kHz linewidth, modulated by a dual-polarization (DP) IQ modulator (IQM). The remaining 30 interfering channels are generated using distributed-feedback (DFB) lasers, modulated (separately for even and odd channels) by a single-polarization (SP) IQM followed by polarization multiplexing emulation (PME), resorting to the use of a polarization beam splitter (PBS), polarization controllers (PC), an optical delay line (ODL) and a polarization beam combiner (PBC). The recirculating loop is composed of 4 spans of pure silica core fiber (PSCF) with 108 km length, 20.12 ps/(nm·km) dispersion parameter and 0.16 dB/km attenuation coefficient. The total link loss, including insertion losses, is 18.75 dB. EDFA-only amplification (5.2 dB noise figure) is used with a spectrally-resolved gain equalizer (GEQ) that compensates for the EDFA gain-tilt and ripples. Finally, a loop synchronized polarization scrambler (PS)

1041-1135 (c) 2018 IEEE. Personal use is permitted, but republication/redistribution requires IEEE permission. See http://www.ieee.org/publications_standards/publications/rights/index.html for more information.

This article has been accepted for publication in a future issue of this journal, but has not been fully edited. Content may change prior to final publication. Citation information: DOI 10.1109/LPT.2019.2906858, IEEE Photonics Technology Letters

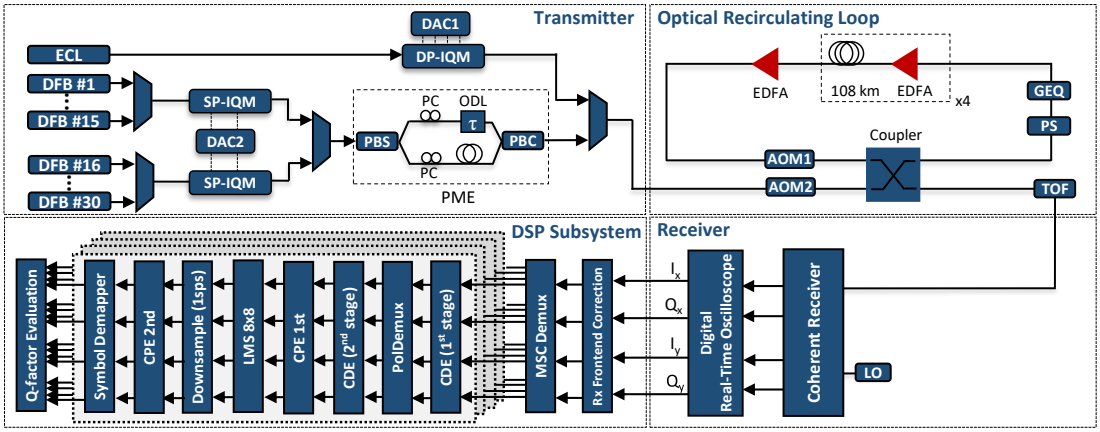

Fig. 3. Experimental setup for long-haul MSC transmission and DSP subsystems.

is applied to statistically average the polarization effects. At the receiver, the CUT is filtered by a tunable optical filter (TOF) and mixed with a local oscillator (ECL with $<$100 kHz linewidth). Finally, the coherently detected signal is sampled by a 50 Gsa/s real-time oscilloscope. Offline DSP is then applied to the stored waveforms, starting with the compensation of the optical front-end imperfections, including Gram-Schimdt orthonormalization, DC component removal and compensation of IQ skew introduced by the receiver. The carrier frequency offset is then estimated digitally and the MSC signal is frequency-demultiplexed into N_{sc} subcarriers. In order to assess the impact of the residual accumulated CD on the performance of Stokes PolDemux, we split the CD equalization (CDE) into two stages. In the first CDE stage, $x\%$ ($x \in [0, 100]$) of the total accumulated CD is compensated, leaving the remaining residual CD at the input of the PolDemux stage, which implements the algorithm described in section II. Then, the second stage of CDE will exactly compensate for the remaining $(100 - x)\%$ of the accumulated CD. This strategy allows to analyze the impact of the residual CD on the performance of our memoryless Stokes PolDemux algorithm, emulating a real condition in which the CD estimation is performed with a given error. Therefore, the only DSP stage that processes a signal with residual CD is the PolDemux stage, while it is guaranteed that the overall system performance is not directly affected by uncompensated CD. Note that the Stokes PolDemux in this study is applied with 2 samples per symbol, using the same implementation scheme originally proposed in [3]. Then, a first coarse carrier phase estimation (CPE) is applied over one of the central subcarriers, using the 16QAM-modified (QPSK partitioning) Viterbi&Viberbi algorithm with 101 taps. The estimated phase noise is then removed from all subcarriers, allowing for the compensation of the transmitter IQ skew with a 51-tap least mean squares (LMS)-driven 8×8 real-valued equalizer [8], initialized in data-aided mode for tap convergence and then switched to decision-directed mode. It is important to mention that all cross-polarization filters in the 8×8 LMS matrix are removed, reducing the total number of individual filters from 64 down to 32. This guarantees that, except for the Stokes PolDemux algorithm, no other DSP subsystems are attempting to perform polarization demulplexing. Also note that the dedicated Stokes PolDemux stage enables the first CPE stage, which avoids the need for an embedded phase tracker within the 8×8 LMS equalizer. After down sampling to 1 sample per symbol, a second V&V CPE stage is applied to each subcarrier with an optimized block length, aimed at the removal of residual nonlinear phase noise, similarly to what has been done in [6]. Finally, symbol demapping is performed and the Q-factor per subcarrier is evaluated from the counted bit-error ratio (BER).

IV. Experimental Results

Applying the DSP chain described in the previous section, the Stokes PolDemux performance is experimentally evaluated for all considered MSC configurations at the optimum launch power of 0 dBm per optical channel [6] and at a fixed transmission distance of 2160 km (5 recirculations). The system performance as a function of the residual CD (bottom x-axis) and the error percentage on CD estimation (top x-axis), after the 1st CDE stage, is shown in Fig. 4a, for a number of subcarriers ranging from 1 to 12. Also, Fig. 4b shows the total residual CD that can be tolerated as a function of the number of subcarriers, assuming a maximum Q-factor penalty (Q_{pen}) of 0.1 dB relatively to the case when CD is fully compensated in the 1st stage. These results clearly show the enhanced tolerance against residual accumulated CD that is enabled by an increasing number of subcarriers. Indeed, for the typical single-carrier signal (1×24 Gbaud) the system is very sensitive to residual CD before the PolDemux stage ($<$ 1 ns/nm is tolerated for $Q_{\mathrm{pen}} \leq 0.1$ dB). Besides, very steep degradation of performance is observed when the CD compensation error is $>$1%, which roughly corresponds to 700 ps/nm of residual CD. By using 2×12 Gbaud, this tolerance is substantially increased to $\sim$10%. In contrast, when the signal is composed of 12 subcarriers (12×2 Gbaud) the system performance remains stable for all range of tested residual CD values, thus enabling Stokes PolDemux to be applied without any prior CD compensation at all (CD is entirely compensated in the second CDE stage, after PolDemux). Taking into account that advanced CD estimation algorithms can typically provide an accuracy

1041-1135 (c) 2018 IEEE. Personal use is permitted, but republication/redistribution requires IEEE permission. See http://www.ieee.org/publications_standards/publications/rights/index.html for more information.

This article has been accepted for publication in a future issue of this journal, but has not been fully edited. Content may change prior to final publication. Citation information: DOI 10.1109/LPT.2019.2906858, IEEE Photonics Technology Letters

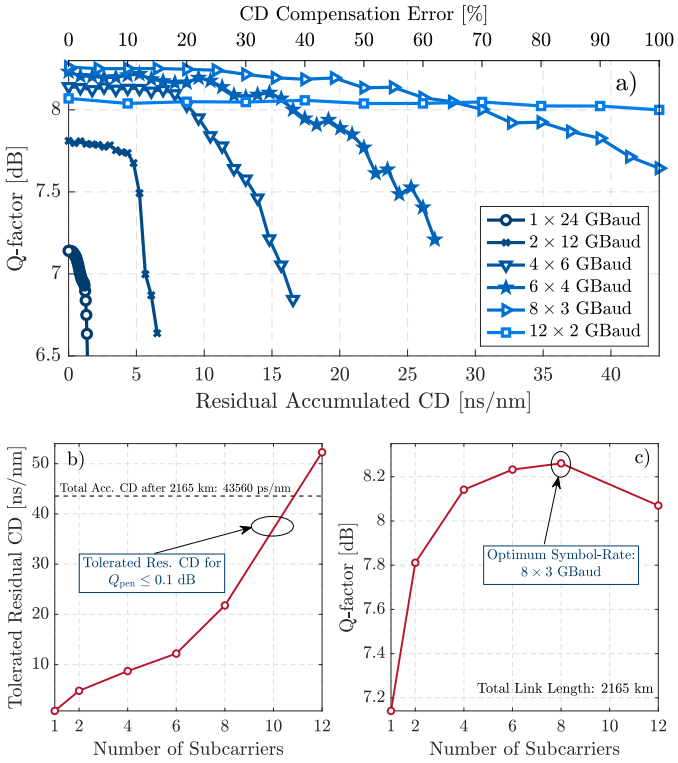

Fig. 4. a) Q-factor vs. residual accumulated dispersion and error percentage on CD estimation after the 1st CDE stage; b) tolerated residual CD (considering $Q_{\text{pen}} \leq 0.1$ dB) vs. number of subcarriers; c) symbol-rate optimization.

of $\pm$300 ps/nm [9], we may conclude that the considered 24 GBaud single-carrier system could still be supported with minimal implementation penalty. Nevertheless, with the current trend towards ultra-high symbol-rates, the margin for CD estimation errors is rapidly closing. Considering the quadratic dependence of the residual CD on the transmitted symbol-rate [7], the tolerated CD values here reported are expected to suffer a $\sim$16$\times$ reduction by increasing the baseline symbol-rate to 100 GBaud, thereby challenging the precision of state-of-the-art CD estimation algorithms. In that case, the use of MSC transmission might become a key enabler for memoryless Stokes-based PolDemux. It is also worth noting that the well-known SRO advantage is still kept using the proposed DSP. This is evidenced in Fig. 4c, which shows the best Q-factor obtained for each MSC configuration, corresponding to the case of perfect CD compensation in Fig. 4a. The optimum symbol-rate is found at 3 Gbaud per subcarrier, providing $\sim$1 dB of gain in terms of Q-factor relatively to the single-carrier case, in accordance with the results from our previous experimental campaign [6].

Besides the enhanced robustness towards residual CD, the use of MSC signals together with Stokes PolDemux can also be advantageous from the complexity point of view. In Fig. 5 we experimentally validate the reduced complexity Stokes PolDemux strategy depicted in Fig. 2 and described in section II, in which the PolTrack stage is only applied over a group of reference subcarriers. The obtained results show that a minimum of 2 to 4 reference subcarriers are needed to achieve the maximum performance (within $<$ 0.2 dB penalty) of

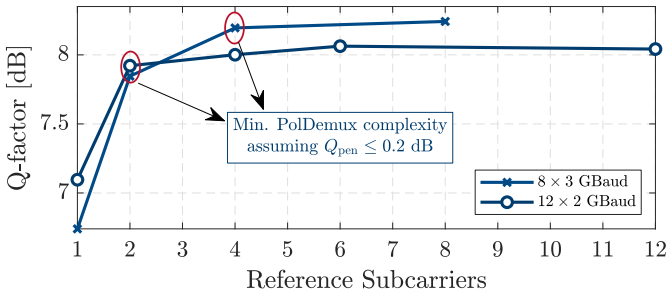

Fig. 5. Impact of the number of reference subcarriers for PolTrack on the overall performance of the Stokes PolDemux algorithm.

the PolDemux algorithm. For the cases of 8×3 Gbaud and 12×2 Gbaud, this roughly corresponds to a computational effort reduction by a factor of 2 and 6 respectively, when compared to an independent Stokes-based PolDemux of all subcarriers. These results show that the frequency-dependent variation of the PolDemux coefficients caused by PMD can be efficiently taken into account without the need to replicate the PolTrack stage over all subcarriers.

V. Conclusions

We have experimentally demonstrated that the adaptive Stokes PolDemux algorithm, which has been previously utilized for short reach ($<$100 km) applications only, can also be efficiently applied to long-haul transmission systems. The enabling factor is the use of MSC modulation, which has been demonstrated to significantly enhance the PolDemux tolerance against residual accumulated CD, thereby potentially allowing for a practical implementation of the modulation transparent Stokes PolDemux algorithm in long-haul scenarios. By restricting the polarization tracking circuitry to a subset of N_{ref} subcarriers, we also demonstrated that the overall PolDemux complexity can be significantly reduced (approximately by a factor of $N_{\text{sc}}/N_{\text{ref}}$) with negligible performance degradation.

References

[1] F. P. Guiomar *et al.*, "Fully blind linear and nonlinear equalization for 100G PM-64QAM optical systems," *J. Lightwave Technol.*, vol. 33, no. 7, pp. 1265–1274, Apr 2015.

[2] S. Savory, "Digital coherent optical receivers: algorithms and subsystems," *Selected Topics in Quantum Electronics, IEEE Journal of*, vol. 16, no. 5, pp. 1164–1179, 2010.

[3] N. J. Muga and A. N. Pinto, "Adaptive 3-D Stokes space-based polarization demultiplexing algorithm," *J. Lightwave Technol.*, vol. 32, no. 19, pp. 3290–3298, Oct. 2014.

[4] S. Ziaie *et al.*, "Experimental assessment of the adaptive Stokes space-based polarization demultiplexing for optical metro and access networks," *J. Lightwave Technol.*, vol. 33, no. 23, pp. 4968–4974, Dec 2015.

[5] M. Qiu *et al.*, "Digital subcarrier multiplexing for fiber nonlinearity mitigation in coherent optical communication systems," *Opt. Express*, vol. 22, no. 15, pp. 18 770–18 777, Jul 2014.

[6] F. P. Guiomar *et al.*, "Nonlinear mitigation on subcarrier-multiplexed PM-16QAM optical systems," *Opt. Express*, vol. 25, no. 4, pp. 4298–4311, Feb 2017.

[7] M. Malekiha *et al.*, "Chromatic dispersion mitigation in long-haul fiber-optic communication networks by sub-band partitioning," *Opt. Express*, vol. 23, no. 25, pp. 32 654–32 663, Dec 2015.

[8] G. Bosco *et al.*, "Impact of the transmitter IQ-skew in multi-subcarrier coherent optical systems," in *Proc. Optical Fiber Communication Conf. and Exposition (OFC)*, no. W4A.5, 2016.

[9] R. Soriano *et al.*, "Chromatic dispersion estimation in digital coherent receivers," *J. Lightw. Technol.*, vol. 29, no. 11, pp. 1627–1637, June 2011.

1041-1135 (c) 2018 IEEE. Personal use is permitted, but republication/redistribution requires IEEE permission. See http://www.ieee.org/publications_standards/publications/rights/index.html for more information.